Rain clutter mitigation based on the Spectral Flatness Measure in surveillance radar

Neuton Severo, Pedro Sega, Leandro Pralon, Bruno Pompeo

***Abstract*— Radar systems are devices mainly used to detect and estimate the kinematic characteristics of targets of interest. Unlike optical sensors, radar systems operate effectively under adverse weather conditions and in the absence of light. Nevertheless, in cases of heavy precipitation, radar performance can be significantly degraded. Reflections from raindrops may generate false targets, while the resulting attenuation can obscure actual targets. To address this, various methods have been proposed for rain clutter mitigation in surveillance radars, most of which rely on stochastic models tailored to specific weather conditions. Unfortunately, any mismatch between the actual weather and the assumed model may significantly impair detection performance. In this context, the present work proposes a model-independent approach to rain clutter mitigation based on the spectral flatness of the received signal. Real data collected from the Brazilian Army's SABER M200 Vigilante radar system were used to validate the proposed method. Its effectiveness in eliminating false targets while preserving true target detections is evaluated, and conclusions are drawn regarding its practical applicability.**

***Keywords*— radar, rain clutter, spectral flatness.**

I. Introduction

In Radar terminology, clutter is a designation given to any object that induces an undesired detection. Such definition depends on the application; for instance, meteorological radars are interested in detecting rain events, whereas surveillance radars need to detect targets despite the rain.

For surveillance systems, clutter can be both stationary as well as non-stationary. Stationary clutters originate from static targets, like mountains or buildings. Non-stationary clutters, on the other hand, are reflecting objects that present some sort of movement, deterministic, or not, like wind turbine, rain, sea and flock of birds, just to cite a few. While the former are easily removed through Doppler filtering methods or Moving Target Indication (MTI) techniques, suppressing the latter is still an open challenge to radar designers [1].

Among the non-stationary clutters that can jeopardize surveillance radar performance, rain clutter is one of the most detrimental. Not only it can appear in any location and at any time but also its behavior is influenced by a large number of variables, being a combination of atmospheric conditions, precipitation characteristics, geographic factors, and electromagnetic interactions. Temperature, humidity, air pressure, and wind speed play a crucial role in the formation and movement of rain, affecting both its intensity and distribution. The size and concentration of raindrops determine how rain interacts with electromagnetic waves while the frequency and polarization of the transmitted signals also affect how rain is detected, with higher frequencies being more susceptible to attenuation and scattering [2].

Unlike modern meteorological radars that use dual polarization to enhance understanding of rainfall characteristics, surveillance systems are generally single-polarized, making it more challenging to handle rain-related targets. Several algorithms have been developed to suppress rain clutter in surveillance radars, most of which are heavily dependent on the chosen stochastic model to characterize it [2, 3, 4, 5]. The traditional Pulse Pairing technique also assumes that rain clutter is stationary, an assumption that proves questionable in many scenarios [1].

Although surveillance systems can benefit from the insights provided by the meteorological community, specially regarding raindrop size distributions and fall velocities [6, 7], the combined factors previously mentioned make rain a highly dynamic and complex phenomenon, posing challenges in developing a one-size-fits-all solution for its removal. Therefore, model independent techniques emerge as alternatives for this problem.

Regardless of the current stochastic models for rain clutter, there is a general consensus that modeling raindrop amplitudes as Gaussian—based on the assumption of multiple independent scatterers and the Central Limit Theorem— may not be the most accurate approach. Therefore, its Power Spectral Density (PSD) is expected to exhibit a non-flat shape, unlike that of pure thermal noise. On the other hand, since rain clutter is indeed characterized by a random process, the presence of a true deterministic target return within a detection cell containing rain clutter is expected to further reduce the spectral flatness. Within this context, in the present work we propose a filtering technique based on the Spectral Flatness Measure (SFM) of the received signal to eliminate rain only detections of an S-band air surveillance system.

The remainder of this manuscript is as follows. Section II describes the radar system used in this work and characteristics of the experiment. Section III provides a characterization of both the signal and the rain clutter data. The rain clutter suppression approach based on the received signal Spectral Flatness Measure is then addressed in Section IV. Finally, conclusions and remarks are presented in Section V.

II. Radar System

The SABER M200 VIGILANTE is a single polarization, medium-range, surveillance radar for air defense, developed by the Brazilian Army Technological Center in collaboration

Neuton Severo, Pedro Sega, Leandro Pralon, Bruno Pompeo, Brazilian Army Technological Center, Rio de Janeiro-RJ, e-mail: severo.neuton@eb.mil.br; This work was partially supported by FINEP.

with Embraer S.A. It employs electronic beam scanning, allowing electromagnetic waves to be directed without the need for mechanical movement. This provides greater agility and flexibility for performing different missions with the same equipment.

The primary radar has 360° coverage, composed of four fixed phased array panels, each covering a 90° azimuth sector. The maximum detection range is 200 km. The system ensures high accuracy, with radial distance estimates under 150 meters and azimuth angle estimates within 5°. By using advanced signal processing techniques, the SABER M200 VIGILANTE radar can detect and determine target cinematic characteristics (azimuth, distance, altitude, and velocity), track trajectories, and classify detected targets. The SABER M200 VIGILANTE is depicted in Fig 1.

Fig. 1: SABER M200 VIGILANTE.

Being a pulse Doppler radar, signals are transmitted every Pulse Repetition Interval (PRI). They interact with the environment and scattered back. The received signals are then processed by the radar to estimate the range, azimuth, and velocity of the targets. Fig. 2 presents the high-level block diagram of the signal processing chain in the receiver.

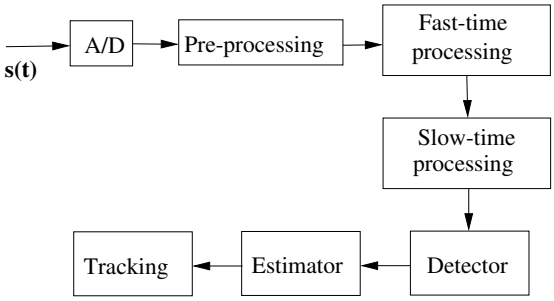

Fig. 2: Block diagram of the signal processing chain in the receiver.

The analog-to-digital (A/D) block is responsible for digitizing the incoming analog signal. The pre-processing block consists of a Digital Down Converter (DDC) followed by decimation. The fast-time processing stage applies a conventional matched filter to the signal, while the slow-time processing stage performs clutter suppression to eliminate stationary returns and enhance moving targets with radial velocity. The output of the slow-time processing is a two-dimensional image commonly referred to as the Range-Doppler Map.

Finally, a Constant False Alarm Rate (CFAR) detector is employed to determine the presence of targets within specific range-Doppler cells. Detected cells are then forwarded to the estimator, which is responsible for extracting the kinematic characteristics of the targets. These estimates are subsequently passed to the tracking module, which is beyond the scope of this work. Pre-processing and detection operations are performed in real-time, typically implemented on an FPGA, whereas estimation and tracking are executed on a CPU.

A. *Experiment*

In this study, data were collected while the radar system was deployed in the city of Campinas, São Paulo, during a rainy day in October 2023. The weather condition was reported by a meteorological radar as shown in Fig. 3, obtained from (https://www.windy.com/). Aircrafts were also present during collection.

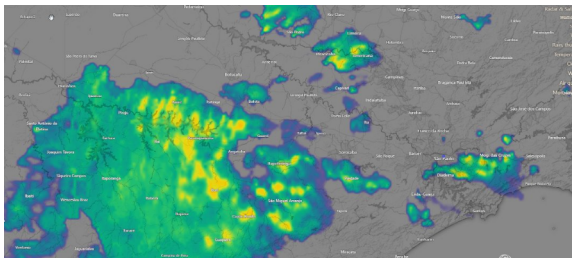

Fig. 3: Rain as detected by a meteorological radar during experiment.

The CFAR output of this rain clutter scenario with targets is illustrated in Fig. 4, where multiple detections are observed. The range-Doppler map is presented in Fig. 5.

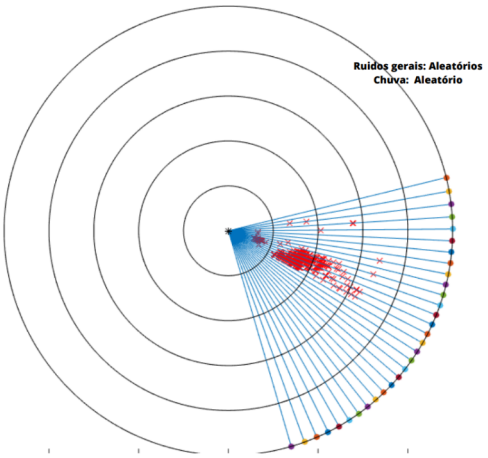

Fig. 4: Detections after CFAR during experiment with rain.

The Range-Doppler map presented in Fig. 5 shows, as expected, that rain clutter is spread across a wide range of distances and Doppler frequencies. As a result, it can both obscure target echoes and trigger an excessive number of detections, leading to an overload in the estimation stage. Consequently, effective mitigation of rain clutter is essential.

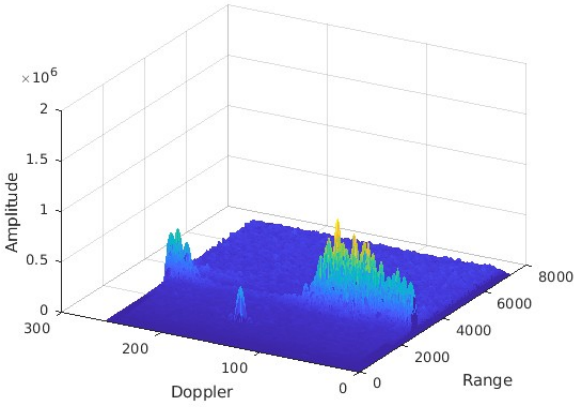

Fig. 5: Range-Doppler map during experiment with rain.

III. Rain Clutter Characterization

Rain is defined as a volumetric clutter, i.e., they are composed by N different scatters (rain drops) within a given volumetric resolution cell. Assuming that each single moving k-th scatterer, is at range R_i (at the time it starts being illuminated by the radar), the complex envelop of the received signal can be written as

$$\tilde{r}(t) = \sum_{k=1}^{N} A_i e^{-j4\pi \frac{R_i}{\lambda}} e^{-j2\pi f_{d_i} t} \tilde{s}(t - T_i), \tag{1}$$

where A_i is a complex term that reflects the backscattering effects, including, the k-th scatterer's Radar Cross Section (σ_i), channel fading, and the gains and distortions introduced by the receiver RF chain, λ is the operating wavelength, f_{d_i} the k-th scatterer's Doppler frequency, associated to its radial velocity, and T_i in (1) represents the time spent by the echo signal to return to the radar, which is given by $T_i = 2R_i/c$, with c being the light speed.

An empirical model for the Radar Cross Section of the k-th scatterer within a rainy volumetric resolution cell [5] is given by

$$\sigma_i = \frac{\pi^5 D_i^6}{\lambda^4} \frac{\epsilon_r - 1}{\epsilon_r + 2}, \tag{2}$$

where D_i is the rain drop diameter and ϵ_r the relative permittivity of water. Several raindrop size distributions have been proposed [8, 9], the Gamma distribution being the most widely spread [2], which is given by

$$N(D, R) = 64500 R^{-0.5} D^2 \exp\left(-7.09 R^{-0.27} D\right) \tag{3}$$

where, $N(D, R)$ represents the number of raindrops with diameter D (in millimeters) per cubic meter of volume, given a rainfall rate R in millimeters per hour (mm/h).

Another strategy to represent the amplitude of rain clutter involves identifying the most suitable Probability Density Function (PDF) that best fits collected data, drawing on knowledge from similar phenomena, such as sea clutter and heterogeneous clutter in high resolution SAR [2]. The complex dynamics of rain lead to non-Gaussian clutter modelling, requiring complex stochastic models for the analysis. Several special cases of univariate stochastic processes (K-compound, Weibull, etc.) have been extensively studied over the years in the sensing community. They all fall in the same class of compound Gaussian distributions which, in turn, had been previously grouped under the SIRP (Spherically Invariant Random Process) family.

SIRP is a multiplicative model that expresses the received signal as a product between the square root of a scalar positive quantity (texture) and the description of an equivalent homogeneous region (speckle), i.e.,

$$r(t) = \sqrt{\tau} z \tag{4}$$

where z is Gaussian with zero mean and τ represents a positive random variable characterizing the spatial variations in the radar backscattering, which is statistically independent of z.

The authors in [2] claim that biparametric generalized Pareto intensity distributions (inverse gamma texture) are recommended to model rain clutter in road traffic surveillance radar at 26.9 GHz, while biparametric K (compound Gaussian distributions, with lognormal textures), are recommended to model rain clutter of millimeter-wave road traffic surveillance radars at 80 GHz. The PDF of the latter, for example, is given by the improper integral

$$f(z; b, \mu) = \sqrt{\frac{2}{\pi\mu}} \int_0^{+\infty} \frac{z}{\tau^2 b} e^{h(z;b,\mu)} d\tau, \tag{5}$$

where

$$h(z; b, \mu) = -\left(\frac{z^2}{\tau^b} + \frac{1}{2\mu} \left(\ln \tau + \frac{\mu}{2} \right)^2 \right),$$

the scale parameter b stands for the mean power of rain clutter, and the inverse shape parameter $\mu > 0$ reflects its degree of non-Gaussianity.

The allegations lead to the conclusion that rain clutter modeling is also highly dependent on the sensor and the environment where it is being used, making it a challenging task trying to find a stochastic model that properly characterizes every possibility. Therefore, model-independent approaches that rely on patterns consistently present in rain clutter represent promising solutions to this problem.

IV. SFM Approach

The Spectral Flatness Measure (SFM) is associated with the entropy rate of a complex stochastic process and serves as an indicator of how information content evolves over time. SFM is traditionally defined as the ratio of the geometric mean to the arithmetic mean of a signal's magnitude spectrum [10]

$$\text{SFM} = \frac{\exp\left[\int_{-\infty}^{\infty} \ln[S(f)] df\right]}{\int_{-\infty}^{\infty} S(f) df} \tag{6}$$

where $S(f)$ is the Power Spectral Density (PSD) of the signal.

Values of SFM close to 1 indicate a random Gaussian signal, while values close to 0 evidence a well structured signal. This behavior is associated to the fact that noise-only observations typically exhibit a flat spectrum, indicating an uniform power distribution across all frequencies. PSD of received signals containing the scatter of targets or even clutter,

on the other hand, generally presents the energy concentrated in specific regions within the PSD, reducing the value of (6) [11]. Therefore, the more prominent a target of interest is immersed in noise, or clutter, the smaller the value of the SFM of the received signal.

Fig 6 presents the SFM of a real received signal composed of a strong rain return between 80 km and 100 km (highlighted in the figure), along with weak targets immersed in noise. It is observed that in the region affected by rain, there is a significant decrease in the SFM value, whereas in regions dominated by thermal noise, the SFM remains approximately constant around a mean value of 0.56.

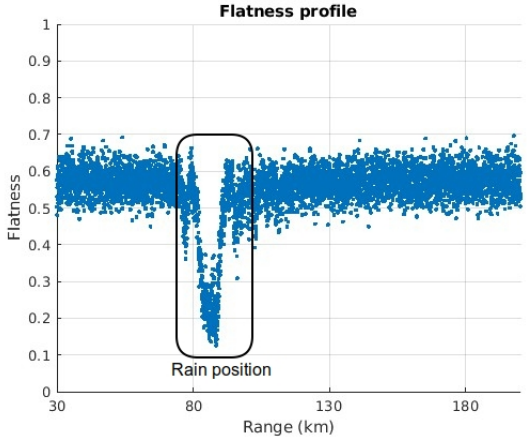

Fig. 6: SFM of a received signal with rain.

The proposed approach is thus to filter data, within the rain scatter region, based on a decision threshold. The threshold can not be too high that no rain is suppressed and not too low that the reflection of strong targets of interest are also removed. Therefore, in order to define which values may provide the best fits, we first evaluated the SFM of a single synthetic target embedded in thermal noise, as a function of its signal no noise ratio (SNR).

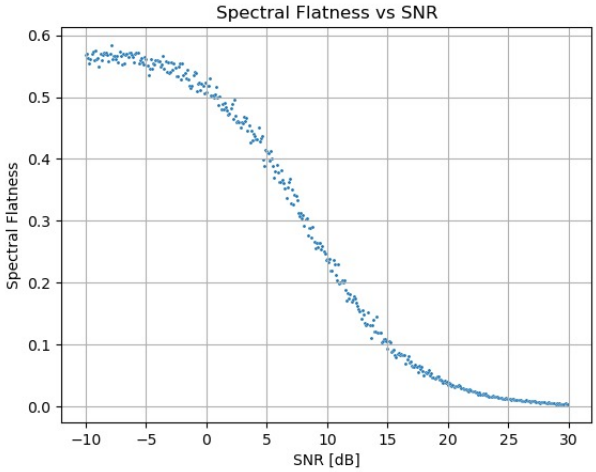

Fig. 7: Spectral Flatness Measures of a signal with one target return immersed in noise for multiples SNR.

Another analysis involved synthetically inserting a target into a burst of received signals varying its SNR. Fig 8 presents the SFM estimated. SFM of the range bin where the target is located is much lower than the ones calculated for range bins composed by noise only or rain clutter returns, leading to a value of SFM close to 0.1.

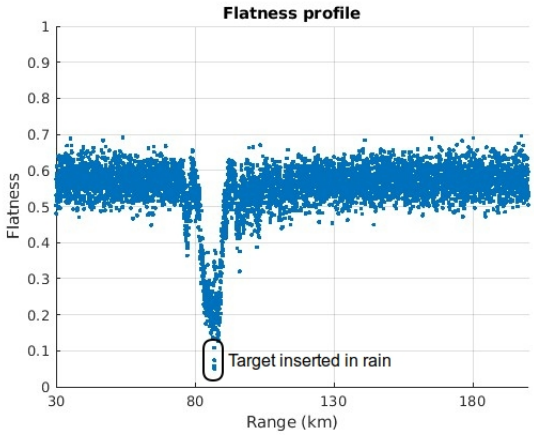

Fig. 8: SFM of a received signal with one single synthetic target added in the signal.

The input SNR of the synthetic target embedded within the rain was varied to assess its impact on the resulting SFM in the corresponding range bin. Fig. 9 shows the estimated SFM as a function of the target's SNR.

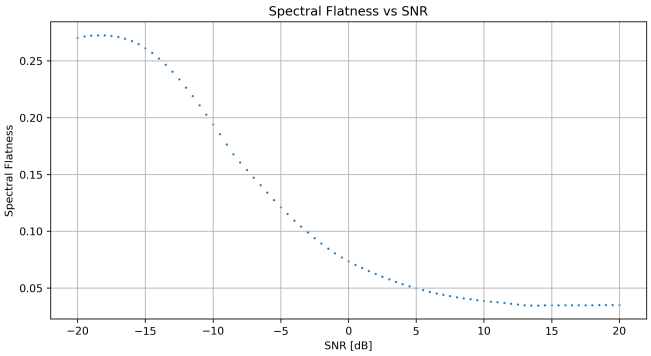

Fig. 9: Spectral Flatness Measures of a received signal with one synthetic target return immersed in noise.

Fig 6 shows that in order to mitigate the entire contribution of rain, an SFM threshold of 0.1 would be necessary. On the other hand,figures 7 and 9 reveals that an SFM threshold of 0.1 will also remove any target with an SNR smaller than 15dB, leaving only the most prominent targets.Consequently, as a practical compromise, we suggest that an SFM threshold of 0.4 serves as a promising starting point for rain clutter mitigation. This threshold significantly attenuates the rain clutter while still allowing the detection of several targets of interest.

V. Concluding Remarks

This article presented an approach to suppress rain clutter in surveillance radar based on the Spectral Flatness Measure of the received signal. Data extraction for the analysis was

performed with an S-Band radar in a rainy day in the city of Campinas-SP.

It was shown that the SFM of noise only, target plus noise and target plus weather clutter and noise present different values, that can be used in a model independent aproach to rain clutter mitigation.

It was also revealed that the choice of the SFM threshold used is crucial for the detector performance and has to be done carefully. Nevertheless such value is a parameter that can be changed easily using a cognitive procedure during operation.

ACKNOWLEDGMENT

The authors would like to thank the Brazilian Development Bank (BNDES), the Financing of Innovation and Research (Finep) and the Brazilian Army for financing and support in making this work possible.

REFERENCES

[1] M.A. Richards, W.A. Holm, and J. Scheer. *Principles of Modern Radar*. Principles of Modern Radar v. 3. SciTech Pub., 2010. ISBN: 9781891121524.

[2] Hai-Long Su et al. “Rain Clutter Modelling and Performance Assessment of Road Traffic Surveillance Radars”. In: *IET Radar, Sonar & Navigation* 19.1 (2025), e70008.

[3] Mohammad Alaee et al. “A new model for rain clutter cancellation in marine radars”. In: *2010 Fourth Asia International Conference on Mathematical/Analytical Modelling and Computer Simulation*. IEEE. 2010, pp. 296–301.

[4] Ilkka Ellonen and Arto Kaarna. “Rain clutter filtering from radar data with Discrete Wavelet Transform”. In: *2006 International Radar Symposium*. IEEE. 2006, pp. 1–4.

[5] Ilkka Ellonen and Arto Kaarna. “Rain clutter filtering from radar data with slope based filter”. In: *2006 European Radar Conference*. IEEE. 2006, pp. 25–28.

[6] Maria A Serio, Francesco G Carollo, and Vito Ferro. “Raindrop size distribution and terminal velocity for rainfall erosivity studies. A review”. In: *Journal of Hydrology* 576 (2019), pp. 210–228.

[7] Walter L Randeu et al. “Raindrop axis ratios, fall velocities and size distribution over Sumatra from 2D-Video Disdrometer measurement”. In: *Atmospheric Research* 119 (2013), pp. 23–37.

[8] AC Best. “The size distribution of raindrops”. In: *Quarterly journal of the royal meteorological society* 76.327 (1950), pp. 16–36.

[9] David A de Wolf. “On the Laws-Parsons distribution of raindrop sizes”. In: *Radio Science* 36.4 (2001), pp. 639–642.

[10] Nilesh Madhu. “Note on measures for spectral flatness”. In: *Electronics letters* 45.23 (2009), pp. 1195–1196.

[11] S Gurugopinath, R Muralishankar, and HN Shankar. “Robust spectrum sensing based on spectral flatness measure”. In: *Electronics Letters* 53.13 (2017), pp. 890–892.